VOL. 25, NO. 2, 2026, 120-137
elektrika.utm.my
EISSN 3083-9394

ELEKTRIKA
Journal of Electrical Engineering

Enhancement of 2D MXene Based Patch Antenna: A Review for Wireless Communication System and Implantable Biomedical Application

Abdur Razzak Khan[1*], **Vinukumar Luckose**[1], **Ariful Islam**[2] and **Noor Farhana Halil Abdul Razak**[3]

[1]Centre for Sustainability in Advance Electrical and Electronic Systems, Faculty of Engineering, Built Environment and Information Technology, SEGi University, 47810 Petaling Jaya, Selangor, Malaysia.
[2]Department of Electrical and Electronic Engineering, Khwaja Yunus Ali University, Enayetpur, Chauhali, Sirajganj-6751, Bangladesh.
[3]School of Engineering, Asia Pacific University Technology and Innovation, Jalan Teknologi 5, Taman Teknologi Malaysia, 57000, Wilayah Persekutuan Kuala Lumpur, Malaysia.

[*]Corresponding author: SUKD2200660@segi4u.my

Abstract: This review delves into the significant advancements in enhancing flexible patch antenna through the integration of two-dimensional transition metal carbide for next-generation wireless communication system and biomedical implantable device. The burgeoning fifth-generation (5G) wireless networks necessitate high performance antenna capable of operating at millimeter to nanometer wave frequencies while accommodating the demand of diverse application. MXene (Ti_3C_2), renowned for its exceptional electrical conductivity, tunable dielectric properties, and mechanical flexibility, emerges as a promising candidate for revolutionizing antenna design. This review comprehensively describes the synthesis techniques employed to produce high-quality MXene, emphasizing the critical role of controlled synthesis in achieving optimal electrical and mechanical properties for antenna integration. Furthermore, this review explores various strategies for incorporating MXene into different components of the patch antenna structure, including the substrate, patch, and transmission line material. The impact of these integration approaches on key antenna performance parameters such as resonance frequency, gain, radiation efficiency, and bandwidth are meticulously analyzed. A significant portion of this review is dedicated to exploring the potential of MXene-based antenna for biomedical applications. The unique properties of MXene, such as biocompatibility and tunability, make them well-suited for developing implantable antenna for a wide range of application. This comprehensive review aims to provide researchers with a valuable resource on the latest advancements in MXene-enhanced patch antenna, fostering further innovation and accelerating the development of next generation wireless communication and biomedical technologies.

Keywords: MXene Antenna, Ti_3C_2, Biomedical Implantable, Biocompatibility, Miniaturization, Pacemaker, Wireless Communication, EMI Shielding

Article History: received 19 April 2025; accepted 12 June 2026; published 31 August 2026
Digital Object Identifier 10.11113/elektrika.v25n2.737

1. INTRODUCTION

The exponential growth of wireless communication systems and implantable biomedical technologies has necessitated the development of advanced antenna designs capable of meeting the demands for high efficiency, miniaturization, and multi-functionality. Patch antennas, with their lightweight, low-cost, and easily integrable nature, have become a cornerstone in modern antenna technology. The large-scale deployment of the Internet of Things (IoT) has significantly increased the demand for enhanced MXene-based patch antennas for application ranging from wireless communication to implantable data transfer interfaces in biomedical fields. To meet this demand, modern antenna design must support high-frequency operation while maintaining compactness and versatility. The development of high-frequency antennas necessitates the seamless integration of radio-frequency (RF) circuits across broad frequency bands to facilitate efficient device-to-device communication [1], [2]. Ultra-thin and flexible MXene-based patch antenna possesses the potential to significantly contribute to these advancements in wireless communication with biomedical applications, as evidenced by recent research findings [3], [4]. A patch antenna comprises a patterned conductive patch, a dielectric substrate, and a ground plane. It can be fed using techniques such as microstrip line, coaxial probe, aperture coupling, and proximity coupling to achieve the desired impedance matching and radiation characteristics [5].

The discovery of MXene has spurred significant research interest in two-dimensional (2D) materials with thicknesses on the order of a few atomic layers, driven by their unique and intriguing properties not observed in their bulk counterparts [6]. MXene materials offer a unique combination of properties that make them highly promising for a wide range of applications in various fields, including energy, electronics, environment, biomedicine and as a medical implantable. In 2D nanomaterials, such as black phosphorous [6], graphene [7], [8] and, MoS_2 [9] are also extensively studied for their prominent behavior with respect to related fields.

The increasing demand for miniaturized and wearable electronics, such as sensors, displays, and data processing devices, has fueled significant interest in the development of ultra-thin and flexible antenna components that ensure dependable wireless connectivity [10], [11]. Ideal materials for these flexible antennas must exhibit a combination of properties, including flexibility, high electrical conductivity, and the ability to withstand mechanical deformation [12]. The performance of an antenna fabricated using thin and flexible conductive metal patches is inherently limited by a fundamental property known as skin depth. According to the skin depth effect, the antenna thickness must be at least a few micrometers to ensure adequate current flow [13]. At higher frequencies, it ensures minimal resistive losses and efficient electromagnetic wave propagation. Dielectric resonator antennas (DRAs) and some metasurface-based antenna do not rely on skin depth, but high performance metals operate on different conductivity principles, which depend on this behavior.

In past decades, the conductive materials such as copper (64.1×106 Sm^{-1}), Chromium (7.9×106 Sm^{-1}), Tungsten (2×107 Sm^{-1}) [14], based materials engaged to design antenna for microwave communication system. For ease of construction, various coating and printing processes are used during antenna fabrication, making the antenna suitable for different dimensions. The 2D conductive materials and some metallic transition metal dichalcogenides have been explored for the manufacturing of printing antennas [13], [15]. In inject printing, the highest electrical conductivity of the printed graphene oxide transmission lines is 2.69×10^{-4} Sm^{-1}, maximum return loss of -36 dB, peak gain 9.6 dB, and efficiency approximately 90% [15], [16], [14]. Because inkjet printing offers quick deposition, excellent resolution, accurate control over the quantity and location of materials deposited, streamlined operating procedures, and non-contact direct printing, it has become more and more popular in a variety of electronic device and RF antenna [13], [15], [17]. Subsequently, a low-temperature processed printable radio frequency identification antenna is also shown to have a thickness of 6 mm and a conductivity of 4.3×10^{4} Sm^{-1} [16]. It has also been exhibited that the metallic 2D $NbSe_2$ thin film is a high-performance sub-micrometer RF antenna, with a sub-micrometer thickness of 0.85 mm and a conductivity of 9.7×10^{5} Sm^{-1} [13], [18]. Again, $Ti_3C_2T_x$ MXene microstrip transmission lines exhibit minimal energy loss, while a 5.5 µm thick MXene patch antenna, fabricated via spray-coating from an aqueous solution, achieves 99% radiation efficiency at 16.4 GHz [19]. This performance rivals a conventional 35 µm thick copper patch antenna, with only 15% of its thickness and 7% of its weight, operating effectively in the 5.6-16.4 GHz frequency range for high-power radiation [19]. Developing the antenna for biomedical purposes depend on its performance and some limitations, such as the interference of biocompatible materials, organs, and tissues [20]. To overcome these limitations, the design of the antenna must incorporate miniaturization, high performance, and the use of materials compatible with the human body. It is crucial for the biomedical wearable and implantable sensors and antennas can transmit and receive remote data from any organs of the human body, and also identify the physiological signs of the patients and received the information accordingly. For miniaturization, patients safety, biocompatibility, low energy consumption, radiation, and a lower frequency band of operation that are effectively noticeable for an implantable antenna [21]. In this case, the antenna selection and fabrication are a challenging matter in the terms of performance and collecting remote signal data from the whole implanted area.

2. OVERVIEW OF MXENE

MXenes are a family of two-dimensional (2D) materials derived from layered transition metal carbides, nitrides, and carbonitrides. Experimental studies have identified more than 50 unique MXene compositions, and the potential for synthesizing an almost infinite number of new chemistries positions MXenes as one of the most versatile material families currently under exploration [22]. The MXene family includes 2D carbides, nitrides, and carbon nitrides, each possessing distinct structural and functional properties. These materials have gained significant attention due to their exceptional features, such as atomic-scale thickness, high metallic conductivity, extensive surface area, and reliable hydrophilicity [23]. MXenes also exhibit outstanding mechanical strength, excellent thermal conductivity, and tunable electronic properties, including a band-gap that can be adjusted from semiconducting to metallic [24].

Table 1. Indicative properties of MXene

Properties	Value	Reference
Electrical conductivity	Up to 20,000 (S/cm)	[25]
Thermal stability	~200-300 °C	[26]
Surface properties	Cr_2C with -OH, -Cl, -F etc	[27]
Dielectric properties	2-20	[28]
Mechanical properties	~20 (GPa)	[29]
Surface plasmon	0.3-1 eV	[25]

Their electromagnetic shielding capabilities and ability to absorb electromagnetic waves have positioned them as promising materials in the fields of 5G communication and EMI shielding. Furthermore, MXenes have demonstrated potential in biocompatibility and environmental applications, including water purification and biosensors. These characteristics make MXenes highly suitable for applications in wireless communication systems, wearable electronic devices, and biomedical implantable technologies. Table 1 summarizes the representative physical and functional properties of MXene materials, including their reported values and corresponding literature sources. The metallic properties of MXenes stem from their unique structure, which consists of (n+1) transition metal layers interspersed with n layers, derived from the selective etching of layered bulk materials [30], [31]. The general formula of MXenes is expressed as Mn+1XnTx. Where,

- M represents transition metals such as Ti, V, Cr, Y, Zr, Nb, Mo, Hf, Ta, or W;
- X denotes carbon (C) or nitrogen (N) and n is 1, 2, 3 and 4;
- Tx refers to surface terminations like -O, -OH, -F, or -Cl, which influence the material's chemical and physical properties.

2.1 MXene Synthesis Procedure

Since the invention of MXenes, research has primarily focused on improving the synthesis of precursor materials such as Ti_3AlC_2, which serves as the precursor to Ti_3C_2Tx. The synthesis process involves etching and delaminating the MAX phase to produce MXene [32]. Especially the MAX phases denoted by M_2XTx, M_3XTx, M_4XTx, and the newer M_5X_4Tx family [22], [30]. Several etching methods have been employed for this purpose, including wet-chemical etching using hydrofluoric acid (HF), HF-containing etchants combined with hydrochloric acid (HCl), and HF-forming etchants that use fluoride salts like LiF, NH_4HF_2, FeF_3, KF, and NaF in combination with HCl [33], [34], [35]. This process yields multilayered MXenes stabilized by van der Waals forces and hydrogen bonding, with surface terminations such as hydroxyl (-OH), fluorine (-F), and oxygen replacing the M-A bonds [36], [37]. Subsequent processing, including centrifugation and controlled sonication, separates solid particles and facilitates the delamination of MXene sheets [38]. Advanced techniques such as molten salt etching using LiF, NaF, or KF, alkali assisted hydrothermal etching, and electrochemical etching in a mixed aqueous solution of LiOH and LiCl have also been developed to enhance the synthesis process [39], [40]. Beyond etching, alternative methods such as ball milling, mechanical force assisted ultra-sonication, and hydrothermal synthesis have been explored to further optimize the production of Ti_3C_2Tx MXene. To improve yield and reduce defects, intercalants are introduced to weaken interlayer bonding, enabling effective mechanical exfoliation into monolayers. Minimally intensive layer delamination (MILD) techniques, which avoid prolonged sonication, are employed to produce larger, higher-quality MXene flakes [41]. Advanced methods, such as using ammonium bifluoride (NH_4HF_2) or organic solvents, further enhance the conductivity and photothermal properties of MXenes [38], making them ideal for high-performance antenna fabrication. These advancements in synthesis techniques have significantly contributed to the scalable production and tunability of MXenes, expanding their potential for various applications [42], [43], [44].

2.2 Material Preparation

The preparation of MXene Ti_3C_2 material involves a standardized process starting with the selection of the MAX phase precursor Ti_3AlC_2. This material, known for its layered structure, is a critical starting point where the "A" layer, in this case, aluminum, is selectively removed to synthesize MXene. The process begins with the etching step, where a fluoride-containing etchant such as hydrofluoric acid (HF), or an in-situ HF solution made by mixing lithium fluoride (LiF) with hydrochloric acid (HCl), is used to remove the aluminum layer [22], [30]. This selective etching breaks the M-A bonds while preserving the M-X structure of the MXene, resulting in the formation of Ti_3C_2Tx [17]. The etching process must be carefully controlled, ensuring that the concentration of the etchant and reaction time are optimized to achieve maximum yield while minimizing damage to the MXene layers. It is crucial to handle HF with utmost caution due to its highly corrosive and toxic nature, adhering strictly to safety protocols. Figure 1 shows the etching method, where the material undergoes a washing and purification process to remove residual etchants and by-products. Deionized (DI) water is used to neutralize the acidic solution, and the washing is repeated multiple times until the pH of the solution reaches neutrality (approximately 6-7) [40], [45]. During this step, centrifugation or filtration is employed to separate the MXene layers from the liquid phase effectively. Proper washing ensures the stability and quality of the MXene material by removing impurities that could otherwise affect its performance.

Once the material is purified, it is dried under controlled conditions to obtain the final product. Drying is typically performed in a vacuum oven at a low temperature, usually between 60 °C and 200 °C [40], [46]. This step ensures the removal of moisture while preserving the layered structure of the MXene. Care must be taken to avoid over-drying, as this could lead to the collapse of the layers or introduce defects in the material. The final step in the synthesis process involves structural and surface characterization of the MXene to confirm its quality and suitability for applications such as 5G communication and biomedical implantable antennas. Various advanced techniques are employed for this purpose. X-ray diffraction (XRD) is used to verify the layered structure and assess the success of the etching process. Scanning electron microscopy (SEM) or transmission electron microscopy (TEM) is employed to examine the surface morphology and determine the thickness of the MXene layers [47]. Energy dispersive X-ray spectroscopy (EDX) is used to confirm the chemical composition and verify the complete removal of the aluminum layer. Additionally, atomic force microscopy (AFM) is applied to analyze the surface smoothness and profile of the material [48]. This rigorous synthesis process ensures the production of high-quality Ti_3C_2Tx MXene with desirable properties such as excellent conductivity, enhanced surface termination, and high structural integrity.

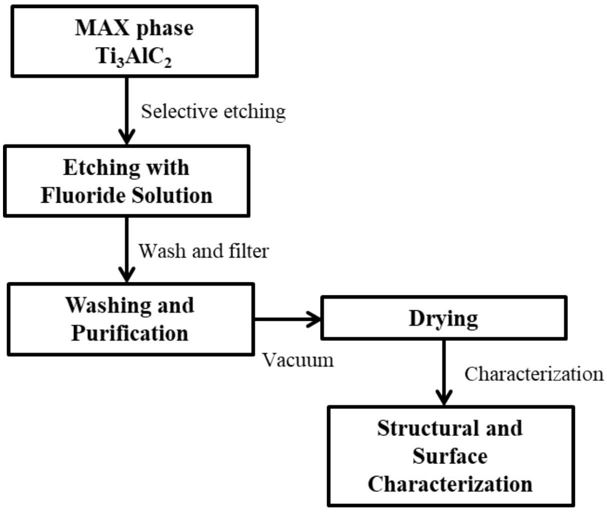

Figure 1. MXene preparation procedure.

2.3 MXene for Antenna Design

MXene is a versatile material in antenna design, functioning either as a conductive layer or as a substrate or filler, depending on the application requirements. As a conductive element, its high electrical conductivity and flexibility enable its use in radiating patches, feeding lines, and wearable or 5G millimeter-wave antennas, including transparent designs with ultrathin films [49]. Alternatively, MXene can be incorporated into polymer composites (such as PDMS or epoxy) to form flexible substrates with tunable dielectric properties, improving impedance matching and electromagnetic performance [50].

Table 2. Impact of MXene properties on micro-strip patch antenna.

Properties	Impact on Antenna Design
High electrical conductivity	Improves efficiency, reduces losses, and enhances gain
Mechanical flexibility	Enables use in flexible, conformal, or wearable antennas
Surface functionalization	Tailors impedance and improves substrate adhesion
Dielectric properties	Allows tuning of frequency and bandwidth.
Thermal conductivity	Ensures heat dissipation, maintaining performance in high-power applications.
Corrosion resistance outdoor or harsh	Enhances durability in environments.
Lightweight and thinness	Ideal for low-profile, portable, and wearable antennas.
Radiation pattern control	Allows design of antennas with specific directional characteristics

Table 2 presents the effect of MXene properties on microstrip patch antenna design, showing how variations in conductivity, flexibility, and dielectric characteristics influence overall antenna performance.

2.4 MXene Based Patch Antenna

Patch antennas are typically designed in rectangular, circular, or triangular geometries based on the desired performance and application requirements. Their thin, planar structure allows patch antennas to fit into confined spaces, making them ideal for wearable or portable devices. A patch design for the back layer on the substrate opposite a ground plane. Generally, a patch becomes a conductive material to fabricate an antenna, while the substrates design to a dielectric material. Patch antennas typically radiate in a single direction, which can improve signal focus and strength in a specific application. Conductive material for antennas is extensively used as a radiating element for its high conductivity. Every highly conductive material ensures high gain, efficiency, bandwidth, and low-cost design and manufacturing. Patch antennas are fabricated in various shapes, each of which plays an important role in optimizing antenna performance for different applications.

At present, MXene-based patch antennas are widely used in 5G wireless communication systems and wearable electronics due to their high integration, flexibility, and ease of use, which make them suitable for compact and high-performance devices [22], [23]. It is composed of a patterned conductive structure that is fed by a transmission line. Antenna performance is commonly analyzed in terms of variations in return loss, radiation pattern, bandwidth, gain, VSWR, and directivity. These variations are influenced by changes in the conductivity and material properties of the patch and ground plane [24]. Quantify the radiation performance of MXene patch are three different techniques, (a) radiation efficiency measurement in reverberation chamber, (b) gain measurement in free space and (c) radiation pattern measurement in an anechoic chamber [19]. Radiation efficiency increases with the thickness of the patch due to a reduction in conductor losses. Additionally, the radiation efficiency of patch antennas tends to be higher at higher frequencies because the substrate's electrical thickness increases with frequency. This leads to a larger amount of radiated fields from the fringing edges of the patch. High radiation efficiency is highly beneficial and applicable for biomedical implantable antenna [51].

Wideband microstrip patch antennas are indeed valuable for biomedical devices, offering advantages in terms of communication reliability and flexibility [52]. The bandwidth of a patch antenna increases with substrate thickness, provided the substrate's material properties are suitable [53]. In the slotting technique, the bandwidth of a patch antenna can be improved by modifying the current distribution and the effective electrical length of the patch [54], [55]. This can be achieved by increasing the overall size of the patch. The antenna design includes a conductive MXene patch, an MXene-based dielectric substrate, and carefully planned geometry on the dielectric surface with a metallic plane on the opposite side [56]. Transmission line and cavity models are important analysis methods for MXene patch antennas [57]. In the case of a rectangular MXene patch, the limiting factors and consistency of current distribution are determined by the patch size and substrate parameters, such as dielectric constant and thickness. MXene rectangular patch antennas are typically narrowband resonant antennas, and their behavior can be modeled using the lossy cavity model, which accounts for material and conductor losses. This model is a suitable choice for analyzing MXene patch antennas in biomedical telemetry applications [58]. A thin MXene dielectric substrate is used for the region in between the patch and ground plane treated as a cavity. The surface field distribution beneath the MXene patch is illustrated in Figure 4 for different geometrical configurations. The variation in geometry significantly influence the electromagnetic behavior of the antenna, particularly the surface current distribution and field concentration. As a result, the antenna performance parameters such as resonance characteristics, bandwidth, and radiation efficiency are affected [59].

The defective ground structure schemes is also enhancing the antenna performance of microwave circuits [60] and improved characteristics. A dielectric substrate and ground plane shows that the great potential challenges owing to their low profile, comfort of manufacturing low cost of volume production and integration with modular circuit [19], [61]. The energy efficient patch antennas have been conventional metals and used to satellite communication system [62], radio frequency identification (RFID) [63], biomedical devices [64], and robotics. In wireless communication application requires the following equation (1-10) to prove the antenna performance. To describes the impedance matching at different operating frequencies and thickness the VSWR in equation (1) necessary to evaluated [65], [66].

$$VSWR = \frac{1+|S_{11}|}{1-|S_{11}|} \quad (1)$$

Where, VSWR is the voltage standing wave ratio between the peak amplitude and the minimum amplitude of the standing wave.

$$w = \frac{C}{2f_0}\sqrt{\frac{2}{1+\varepsilon_r}} \quad (2)$$

Where, w is patch width, ε_r is the dielectric constant, f_o is the resonance frequency and C is the speed of light ($3 \times 10^8 cm/sec$) in equation (2).

$$L = L_{eff} - 2\Delta L \quad (3)$$

Where, Length of patch is L, effective length L_{eff} and extension of length is ΔL in equation (3) [66].

Therefore,

$$L_{eff} = \frac{C}{2f_0}\sqrt{2\varepsilon_{eff}} \quad (4)$$

Here the substrate's effective dielectric constant is ε_{eff}.

$$X_f = \sqrt{\frac{L}{\varepsilon_{eff}}} \quad (5)$$

$$\text{And } Y = \frac{w}{2} \quad (6)$$

Where, X_f is the input position along with x axis and Y_f is the input location along with y axis.

$$\Delta L = 0.412\frac{(\varepsilon_{eff}+0.3)(\frac{w}{h}+0.264)}{\varepsilon_{eff}(\varepsilon_{eff}-0.258)(\frac{w}{h}+0.8)} \quad (7)$$

Where, ΔL is the length extension.

$$\varepsilon_{eff} = \frac{(\varepsilon_r+1)}{2} + \frac{(\varepsilon_r-1)}{2}(1+12\frac{h}{w})^{0.5} \quad (8)$$

$$\text{Length of ground plane, } L_g = 6h + L \quad (9)$$

$$\text{Width of ground plane, } w_g = 6h + w \quad (10)$$

3. ANTENNA FABRICATION PROCESS

3.1 Inkjet Printing

Inkjet printing is a direct write technique that allows for precise deposition of MXene inks onto substrates. In this method, a digitally controlled print head ejects small droplets of MXene ink onto the substrate, layer by layer, to create the antenna structure. Figure 3 shows the inkjet printing process for manufacturing an antenna. The process is highly adaptable, allowing for flexible designs that can conform to various surfaces, which are particularly valuable in wearable or implantable devices [67]. Inkjet printing processes can be classified into two main categories based on how ink is delivered to the substrate. One is continuous inkjet (CIJ) printing, where ink droplets are continuously generated and either directed to the substrate or deflected into a gutter for recirculation. It is commonly used in high-speed industrial or packaging applications [68]. Another one is Drop-on-Demand (DOD) inkjet printing, which has revolutionized material synthesis by enabling precise, additive deposition of functional materials across various advanced applications [69]. In electronics, it is widely used for fabricating flexible and wearable devices, including RFID antennas, MXene-based patch antennas, and printed circuit boards (PCBs), offering a cost-effective alternative to traditional photolithography [70]. In biomedical fields, it facilitates the production of biosensors, drug delivery systems, and implantable antennas due to its ability to print biocompatible materials at room temperature.

3.2 Spray Coating

Spray coating is a versatile method for fabricating antennas by depositing a fine mist of conductive material onto a substrate. Figure 3 shows the spray coating technique for the fabrication of an antenna. This technique offers advantages like versatility in substrate choice, flexibility in creating complex patterns, low cost, high-throughput production, and the ability to coat conformal surfaces [17]. Spray coating is widely used in applications such as wearable electronics, the Internet of Things, medical implants, automotive, and aerospace, enabling the creation of antennas on various materials like fabric, plastic, and even curved surfaces [71].

3.3 Screen Printing

Screen printing is a cost-effective method for fabricating antennas, particularly for high-volume production. It involves transferring conductive ink through a mesh screen onto a substrate, creating the desired antenna pattern [72]. This technique is versatile, compatible with various substrates and inks, and enables rapid production of antennas. Screen printing is widely used in applications like RFID tags, wearable electronics, automotive components, and medical implants, offering a cost-effective and efficient way to integrate antennas into a broad range of devices [73], [71].

The fabrication process of the textile-based antenna begins with screen printing conductive silver ink (DuPont 5064 H) onto nonwoven fabrics to create the patch and ground layers shows in Figure 2 (a). A vinyl mask ensures high-resolution patterns for transmission lines and gaps, while the printed fabric is cured at 130°C for 15 minutes to ensure durability. For the dielectric layer in Figure 2 (b) and (c) represents the barium titanate (BT) UV-curable dielectric ink is spray-coated onto a knit fabric substrate consisting of six layers laminated with thermoplastic polyurethane (TPU) webs, effectively modifying the dielectric constant. The final assembly in Figure 2 (c) involves laminating the patch and ground nonwoven layers with the BT-coated knit fabric layers using TPU webs, while an additional TPU layer encapsulates the structure for protection. The completed antenna is flexible, durable, and capable of effective signal transmission, as demonstrated in the final product image as Figure 2 (d) [74].

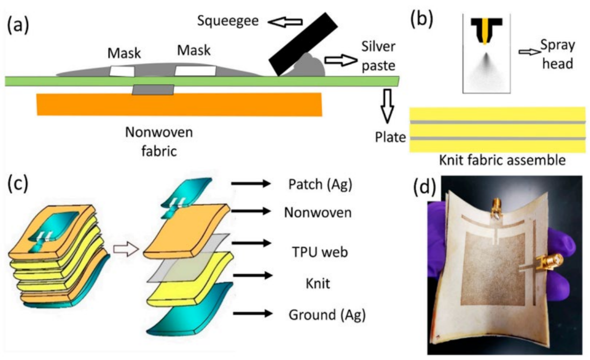

Figure 2. Fabrication of wearable textile based antenna. (a) Screen printing by silver paste for the patch and substrate. (b) Spray coating process of barium titanate (BT) onto the knit fabric substrate. (c) Two layers of nonwoven fabric and six layers of knit fabric spray coated of BT dielectric ink, and finally (d) fabricated the wearable textile-based antenna [74].

3.4 Etching

Etching is a subtractive technique where unwanted material is removed from an MXene-coated surface to define the antenna pattern. There are two main types of etching, such as chemical and plasma etching [75]. In chemical etching, a pattern is created by applying a masking layer, followed by exposure to an etchant that selectively removes unprotected areas. Plasma etching, on the other hand, uses a plasma source to remove material in a controlled manner, achieving finer resolution. Etching offers high precision and is well-suited for producing antennas with intricate geometries and fine details [76]. Plasma etching, in particular, is capable of achieving nanoscale features, which is beneficial for creating a miniaturized antenna. The process can be complex, as it often requires multiple steps, including masking, exposure, and washing [22]. Chemical etching can involve hazardous materials, requiring careful handling and disposal, while plasma etching typically requires specialized equipment.

3.5 Sputtering

Sputtering is a deposition process that involves bombarding an MXene target material with high-energy particles in a vacuum environment, causing atoms or molecules to be ejected and deposited onto the substrate [41]. This creates a thin, uniform layer of MXene, which can then be patterned to form the antenna. The thickness and quality of the deposited layer can be controlled by adjusting the sputtering parameters, such as power, duration, and gas composition. Sputtering produces highly uniform and dense films, making it suitable for application that require high-performance [77]. It also produces even, thin coatings, which are ideal for creating MXene antennas with consistent signal transmission. The thickness and quality of the coating can be finely tuned by adjusting sputtering parameters, making it adaptable for different antenna requirements. The technique is also versatile, as it can be used to coat a variety of substrates, including flexible and non-flat surfaces.

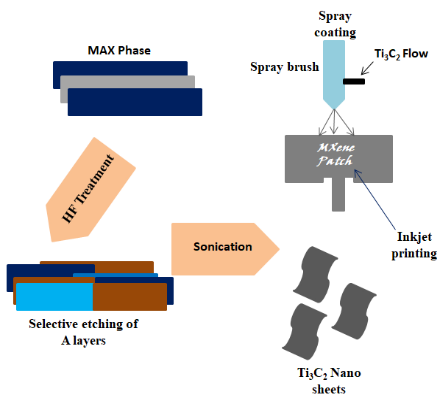

Figure 3. Different types of MXene material sheets

Figure 4 emphasizes the versatile application of Ti_3C_2 MXene as a high-performance material for a 5G antenna system, highlighting its integration into patch, substrate, and transmission line components for optimal signal propagation and miniaturized design. Figure 4 also illustrates the design and integration of MXene materials for antenna applications, showcasing their utilization in different configurations and components. Figure 4 (a) highlights the use of MXene as a patch, substrate, and transmission line material for an antenna design. The ground surface supports the MXene-coated substrate, while the MXene patch acts as the radiating element, and the transmission line facilitates signal input or output. This configuration demonstrates the adaptability of MXene materials in providing excellent conductivity and compatibility with antenna structures.

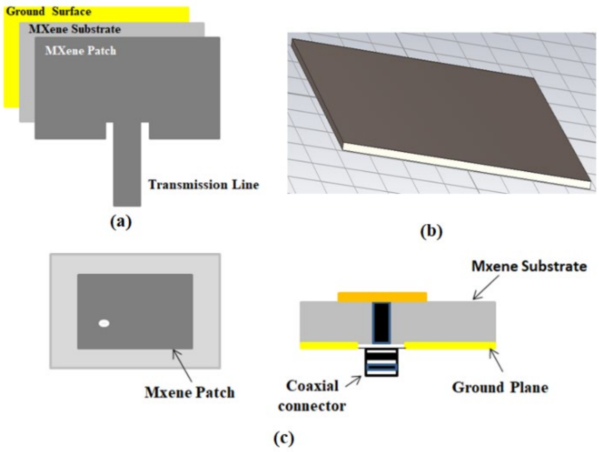

Figure 4. (a) Characteristics of MXene coating as a patch, substrate, and transmission line material, (b) substrate design in CST by Ti_3C_2 MXene, (c) co-axial connection between different surfaces.

Figure 4 (b), the three-dimensional substrate design modeled in CST software employs Ti_3C_2 MXene as the substrate material. The substrate is represented as a uniform, layered block, emphasizing its structural role in supporting the antenna's radiating elements and maintaining the integrity of the design. Figure 4 (c) shows the co-axial connection details the interface between different surfaces within the antenna system. The MXene patch is mounted on the MXene substrate, which is separated from the ground plane. The coaxial connector bridges the input signal to the patch while maintaining the electrical isolation of the ground plane. This configuration illustrates the precise alignment and electrical continuity required for effective antenna performance, exploiting MXene's excellent electrical and mechanical properties.

4. MXENE PATCH ANTENNA AND EMI SHIELDING

Integrating MXene in a patch antenna is a promising approach to improve performance, especially in applications demanding high conductivity and mechanical flexibility. MXene's metallic nature allows for effective signal conduction and minimal energy loss. In biomedical application MXene based patch antennas could enable effective wireless communication with compact, implantable devices, enhancing diagnostic and therapeutic capabilities [78]. This adaptability of MXene to varying condition and customizable electronic properties continues to drive research into optimizing MXene-based patch antennas for high-frequency and high-performance wireless communication. The surface chemistry of MXene is highly tunable, as it can have different functional groups that influence its electronic properties. This ability to adjust the surface functionality allows fine tuning of MXene electrical and dielectric properties to meet the specific needs of wireless components, including impedance matching for improved antenna performance. Additionally, by adjusting the MXene structure and composition, it's possible to optimize them for specific frequency ranges used in wireless communications, enhancing the efficiency and bandwidth of antenna and RF devices. Table 3 summarizes the properties of various antenna configurations, highlighting differences in design, material selection, and operational characteristics. These comparisons are essential for optimizing antenna performance in diverse communication and sensing applications for MXene. MXenes offer exceptional benefits as materials for electromagnetic interference (EMI) shielding due to their high electrical conductivity and layered structure [79]. Their conductive nature enables them to absorb or reflect electromagnetic waves effectively, preventing unwanted signals from interfering with electronic devices. This is particularly valuable in applications where signal clarity is essential, such as wireless communication and high-frequency electronics.

Table 3. Comparative antenna and its properties

Antenna	Materials	Frequency (GHz)	Ref.
MXene patch (5.5) µm	Ti_3C_2, copper	5.6 to 16.4	[19]
MXene dipole (~100) nm	Ti_3C_2	2.4	[17]
MXene monopole (5.5) µm	Ti_3C_2	1.7 to 4.0	[80]
Rectangular patch (80× 80×3.31) mm^3	MWCNT	7.29	[81]
Antenna array (10 × 9 × 1.26) mm^3	Graphene	26.0	[82]

Additionally, MXene thin and flexible nature makes them ideal for creating lightweight, conformable shielding solutions that can easily integrate into compact and flexible devices, including wearable and biomedical implants [83]. Overall, MXene-based EMI shielding enhances device performance by minimizing interference, protecting sensitive electronics, and supporting clearer signal transmission in complex environments [84]. MXenes, when appropriately processed and protected from oxidation, can demonstrate stability in a range of environmental conditions. For applications of biomedical devices and flexible electronics, MXenes' stability is essential for long-term performance.

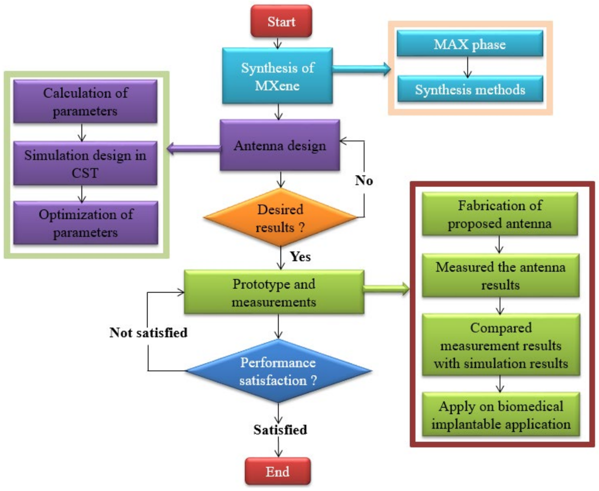

Figure 5. Block diagram of proposed MXene based patch antenna.

5. IMPORTANCE OF ANTENNA IN IMPLANTABLE APPLICATION

MXene holds significant promise for biomedical implantable antennas due to its unique combination of properties. Their high electrical conductivity allows for efficient signal transmission, crucial for reliable communication between implanted devices and external systems. Furthermore, the flexibility and biocompatibility of certain MXenes make them suitable for integration with biological tissues, minimizing adverse reactions. This is very important when considering implanted devices. The ability to fabricate thin, flexible antenna with MXene enables the development of miniaturized and conformable implants, improving patient comfort and devices functionality. In essence, MXene offer a pathway to create next-generation biomedical implantable antenna with enhanced performance and biocompatibility.

5.1 Impact of MXene Properties on Biomedical Application

The fabrication of antennas for human and animal bodies presents significant challenges. The design of high-performance implantable MXene antennas requires careful consideration of their surface area in various orientations, on-body, off-body, and in-body-centric. This antenna is intended to detect abnormal conditions of organs via wave signals. However, synthesized materials often face limitation due to their properties. MXene Ti_3C_2, a high-performance material, has gained attention in the biomedical field for its antibacterial activity and superior thermal and electrical properties. The unique structural features of MXene, including its high specific surface area, excellent physiochemical properties, high photo thermal conversion efficiency, and particularly its antibacterial properties, make it highly applicable for biomedical implantable antenna.

5.2 Potential Benefits of Implantable Antenna

Implantable antennas offer significant advantages in biomedical monitoring systems, particularly for continuous and real-time health assessment. These devices enable improved monitoring by providing continuous physiological data, such as organ function parameters, which assists in the early detection of abnormalities and timely medical intervention. With the integration of IoT-based healthcare systems, implantable antennas facilitate reliable real-time data transmission for remote patient monitoring and clinical decision-making [85]. Furthermore, they help reduce the need for invasive diagnostic procedures, such as biopsies, thereby minimizing patient discomfort, lowering surgical risks, and improving overall healthcare efficiency.

5.3 Miniaturization

The miniaturization of antennas in biomedical implantable devices is essential for ensuring efficient wireless communication while maintaining a compact size to minimize patient discomfort and surgical complexity. Due to the limited space and biocompatibility requirements, implantable antenna must be designed with high efficiency, low power consumption, and stable performance in the human body. Techniques such as metamaterials, high-permittivity dielectric substrates, fractal geometries, and substrate-integrated waveguides are commonly used to achieve miniaturization without compromising performance [86]. Additionally, materials like biocompatible polymers and flexible MXene-based structures are explored to enhance durability and integration with body tissues. These miniaturized antennas facilitate real-time health monitoring, data transmission, and energy harvesting for implantable medical devices [87], making them a crucial component in modern biomedical technology [88].

5.4 Implantable Antenna for Kidney Disease

Implantable antenna for kidney disease is a developing area of research, with the potential to revolutionize the way chronic kidney disease (CKD) is managed. These antennas are designed to be placed inside the body, typically in the abdomen, underneath the skin or near the kidney, and can be used to wirelessly transmit data about the kidney's function and health to an external device [89]. This data can then be used by doctors to monitor the patient's condition and make treatment decisions. For patients with chronic kidney disease (CKD) requiring hemodialysis, Arteriovenous Grafts (AVGs) are crucial for survival [90]. Unfortunately, these grafts frequently experience postoperative complications like restenosis (cellular accumulation), blood clots, and infection [91]. These complications are major contributors to patient illness and death. Next-generation hemodialysis implants, incorporating biosensors and multi-band antennas for wireless power and data transmission, offer a promising solution [85]. These advanced implants could monitor specific disease indicators and assess AVG patency, revolutionizing CKD care. Table 4 presents a summary of implantable antennas for kidney disease monitoring, including key parameters such as antenna type, materials used, and operating frequency (GHz). The table highlights the selection of biocompatible materials and suitable frequency bands to ensure safe and efficient in-body communication. As shown in Table 4, most designs focus on miniaturization and optimal frequency selection to achieve reliable performance while minimizing signal attenuation within biological tissues.

Figure 6 showcases the smart architecture of AVGs integrated with an implantable antenna system designed for kidney monitoring. The device features several components, including a battery for power, a smart graft for advanced vascular performance, an encapsulation shell for biocompatibility, and protection of internal electronics [85].

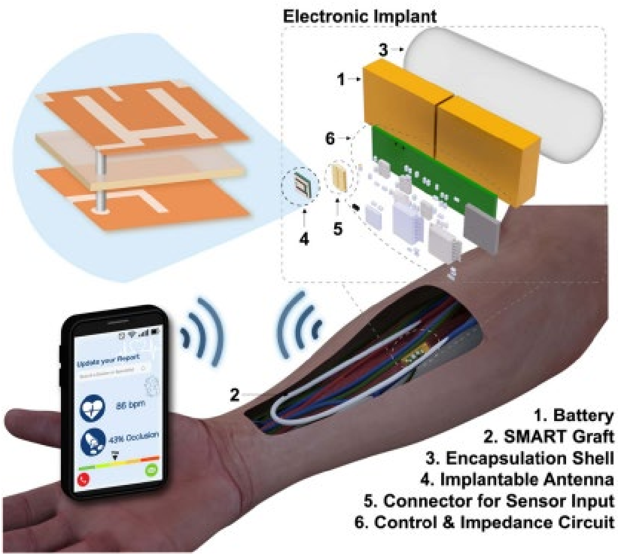

Figure 6. Smart architecture of Arteriovenous grafts [85]

The implantable antenna enables wireless communication with external devices, such as a smartphone, which displays real-time health data, including heart rate and occlusion percentage. A connector interfaces with sensors that gather physiological data, while the control and impedance circuit processes this information for efficient monitoring. This innovative system allows for continuous, non-invasive health tracking, providing critical insights for patients undergoing kidney treatment, such as dialysis, enhancing care efficiency and patient outcomes.

Table 4. Implantable antenna for kidney disease

Antenna	Materials	Frequency (GHz)	Ref.
Dual band fractal (9. × 59.5× 0.635) mm^2	FR4, Rogers RT5880	1.4, 2.45	[92]
MIMO Cubic (15× 15× 15) mm^2	RT Duroid 5880	2.45, 5.8	[93]
Wide band patch (7.5×7.5×1.27) mm^2	RO3010	2.45	[94]
Dual-band patch (5 ×5× 0.635) mm^3	Rogers RT5880 and FR4	2.4, 2.45	[85]

5.5 Implantable Antenna for Heart Disease

Wireless transmission of heart function data is achievable through a tiny, surgically implanted antenna located in the chest cavity. This antenna sends information to an external device, providing continuous cardiac monitoring for patients with heart condition [95]. Often integrated with implantable cardiac devices like pacemakers and cardioverter defibrillators (ICDs), this technology supports remote monitoring, decreasing reliance on wired systems and hospital visits [20].

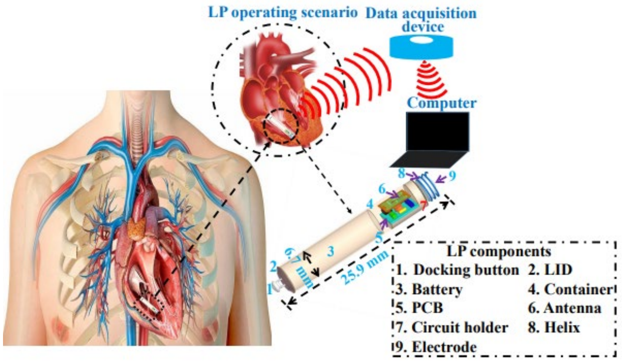

Figure 7. Antenna behavior as in leadless peacemaker [96]

Figure 7 depicts the operating scenario of a Leadless Pacemaker (LP) and its components, showcasing its function in regulating heart rhythm for patients with cardiac disorders. The pacemaker is implanted directly into the heart, where it delivers electrical pulses to maintain a stable rhythm [97]. It communicates wirelessly with a data acquisition device, which transfers information to a computer for real-time monitoring and analysis [95]. Table 5 provides a comprehensive summary of implantable antennas developed for cardiac disease monitoring, incorporating key parameters such as antenna configuration, constituent materials, and operating frequency (GHz). The comparison highlights the critical role of biocompatible materials and appropriate frequency selection in ensuring reliable in-body communication within the cardiac environment. As illustrated in Table 5, recent designs primarily focus on antenna miniaturization, low specific absorption rate (SAR), and stable electromagnetic performance, which are essential for safe, continuous monitoring and efficient data transmission in advanced cardiac healthcare systems. The compact design (25.9 mm) includes several components, a docking button for implantation, a lid and container for biocompatibility and protection, a battery for power, a PCB (Printed Circuit Board) for electronic circuitry, an antenna for wireless communication, a circuit holder for stability, a helix for anchoring to heart tissue, and an electrode for delivering electrical impulses [96]. This leadless design reduces surgical risks and enhances patient care through continuous cardiac monitoring and remote data analysis.

Table 5. Implantable antenna for cardiac disease

Antenna	Materials	Frequencies (GHz)	Ref.
Ultra-wide Bandwidth (6 × 6.2 × 0.254) mm^3	Rogers RT/ Duroid 6202	1.4	[96]
Dual band conformal (6 × 6 × 0.254) mm^3	Rogers RT/ Duroid 6010 LM	1.4, 2.45	[98]
MIMO (3.4 × 6.6 × 0.254) mm^3	Rogers 6010LM	2.4, 5.8	[99]
Patch (8.6×8.6×4) mm^3	Rogers RO 6010, ceramic alumina	2.4	[100]

6. RF PROPAGATION

6.1 RF Propagation in the Lossy Medium

The properties of radio waves are largely determined by the medium's permeability, permittivity, and conductivity, with equation (11) describing an electromagnetic wave moving in the Z-direction [101].

$$E = Ee^{\gamma z} \qquad (11)$$

The wave amplitude in the z-direction is given by E, and γ defined by equation (12), represents the complex propagation constant. As indicated by equation (11), the gradual increase in the complex propagation value leads to the attenuation of electromagnetic waves in the inhomogeneous area.

$$\gamma = j\omega\sqrt{\mu\varepsilon} \qquad (12)$$

Where, $\mu = \mu_r\mu_0$ that refers the permeability of the medium, $\mu = \mu_0$ the $\mu_r = 1$, for biological materials and relative permittivity is $\varepsilon = \varepsilon_r\varepsilon_0$.

The relative permittivity of a lossy medium is complex due to the influence of the medium's conductivity, which affects its ability to store and dissipate energy [103]. The real part of permittivity reflects the material's capacity to store electric energy, while the imaginary part, influenced by conductivity, represents energy lost as heat. This result in electromagnetic wave attenuation as part of the wave's energy is absorbed and dissipated, impacting propagation, reflection, and absorption within the medium. The relative permittivity is described as in equation (13) [102],

$$\varepsilon(\omega) = \varepsilon'(\omega) - j\varepsilon''(\omega)$$

$$= \varepsilon_r'(\omega)\varepsilon - j\varepsilon_r''(\omega)\varepsilon_0 \qquad (13)$$

Here, the real part and imaginary of relative permittivity are Ɛ′ and Ɛ′′ as in express in equation (13), and the imaginary part are obtain from equation (14) and (15),

$$\varepsilon_r''(\omega) = \frac{\sigma}{\omega\varepsilon_0} \qquad (14)$$

$$\tan\delta = \frac{\varepsilon_r''}{\varepsilon_0'} \qquad (15)$$

The complex propagation constant is a key parameter for understanding wave behavior in implantable antennas within biological tissues. It characterizes how electromagnetic waves propagate, attenuate, and phase shift as they travel through a medium, which in this case, is the human body. The complex propagation constant is obtained from equations (12) and (13) [102].

$$\gamma = j\omega\sqrt{\mu\varepsilon'\sqrt{1 - j\frac{\sigma}{\varepsilon'}}} \qquad (16)$$

$$\alpha = \omega\sqrt{\frac{\varepsilon_0\mu_0\varepsilon_r'}{2}\left(\sqrt{1+\left(\frac{\sigma}{\omega\varepsilon_0\varepsilon_r'}\right)^2} - 1\right)} \qquad (17)$$

$$\alpha = \omega\sqrt{\frac{\varepsilon_0\mu_0\varepsilon_r'}{2}\left(\sqrt{1+\left(\frac{\sigma}{\omega\varepsilon_0\varepsilon_r'}\right)^2} + 1\right)} \qquad (18)$$

Where, the attenuation constant α in equation (16) represents the loss of wave amplitude due to energy absorption by the medium and material conductivity, and in imaginary part, the phase constant β in equation (17) describes the change in phase of the wave as it propagates through the medium, these are combine to form the complex propagation constant γ in equation (18), respectively.

6.2 Propagation Speed in Human Body

The propagation speed of electromagnetic waves inside the human body depends on the dielectric properties of the tissues, including the relative permittivity and conductivity. These properties vary across different tissues such as fat, muscle, skin and influence the wave velocity and attenuation [104].

The propagation speed is given by,

$$\upsilon = \frac{c}{\sqrt{\varepsilon_r'}} \qquad (19)$$

Where, c is the speed of light in a vacuum and ε_r' is the real part of the complex relative permittivity of the tissue.

6.3 Impact of Effective Wavelength

The impact of effective wavelength reduction on implantable antenna performance requires careful consideration of tissue type, operating frequency, and antenna geometry. Accurate modeling of ε_r, and λ_{eff} ensures reliable performance for application [64]. The equation of effective wavelength is,

$$\lambda_{eff} = \frac{2\pi}{\beta} \qquad (20)$$

The relationship between effective wavelength λ_{eff} and, phase constant β helps determine antenna dimension and placement within the body. Higher frequencies result in higher β values and shorter λ_{eff} affecting signal strength and coverage.

6.4 Radiated Power (P_r)

The radiated power of an antenna is the power emitted as electromagnetic radiation into the surrounding medium [105]. For a lossy medium, the radiated power is affected by the dielectric and conductive losses of the medium.

$$P_r = P_{input}(1+|S_{11}|)^2 \qquad (21)$$

Where, P_{input} is the input power delivered to antenna and $|S_{11}|$ is the mismatch between the antenna, and its environment.

6.5 Biocompatibility of MXene

The biocompatibility of MXene patch antenna for biomedical application is a fundamental requirement, as these devices are intended to function in close contact with or inside human tissues. MXenes, a family of 2D transition metal carbides and nitrides, possess exceptional properties such as high electrical conductivity, flexibility, and tunable surface chemistry, making them promising candidates for implantable antennas. However, ensuring their compatibility with biological systems involves addressing several critical factors. One of the primary concerns is cytotoxicity. MXenes, such as Ti_3C_2Tx, exhibit varying levels of cytotoxicity depending on their size, surface chemistry, and concentration. Surface functionalization with groups like -OH, -O, and -F can enhance hydrophilicity, minimize toxicity, and improve their interactions with biological systems [105]. Studies suggest that low concentrations of MXenes are generally non-toxic to cells, but higher doses or improper functionalization can generate reactive oxygen species (ROS), which may cause oxidative stress and cellular damage [106]. Figure 8 shows an implantable futuristic bio-integrated antenna, designed for a data transfer interface from internal organs and communication with an external system. It's refers to the concept of combining biological systems with antenna technology, creating designs that are not only efficient for communication but also seamlessly integrated with living organisms or biological systems.

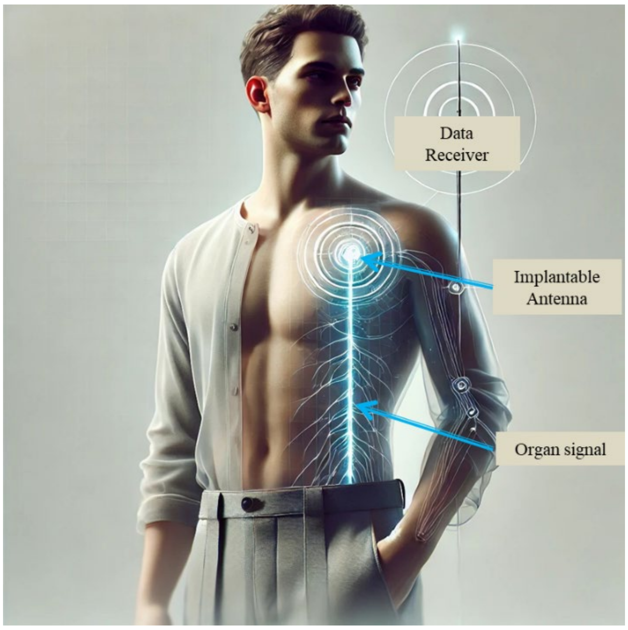

Figure 8. Futuristic bio-integrated design of antenna

This could involve embedding antennas into living tissues, plants, or even using biological materials to form parts of the antenna itself.

6.6 Encapsulation and durability

Encapsulation and durability are crucial factors for the long-term success of an antenna. It serves as a protective barrier to prevent direct exposure of materials to body fluids, which can cause degradation or oxidation. MXene (Ti_3C_2) is susceptible to oxidation when exposed to moisture and oxygen in the body, potentially leading to the release of harmful ions or particles that could interact adversely with tissues [107]. To mitigate this, encapsulation with biocompatible materials such as Parylene-C, polydimethylsiloxane (PDMS), or other polymer coatings is often used [108]. These materials provide a stable, non-toxic interface that prevents oxidation and corrosion, extending the operational lifespan of the antenna and enhancing its overall biocompatibility. Encapsulation also prevents leakage of conductive materials and protects against immune responses, reducing the risk of an inflammatory reaction. Durability is another key consideration, as the antenna must withstand various mechanical stresses, including bending, stretching, and vibrations, especially when embedded in soft tissues or on flexible substrates like skin [109].

6.7 Degradation and Stability

Degradation and stability are equally critical for the long-term use of an antenna in vivo [110]. Degradation refers to the gradual decline in an antenna's functionality over time due to factors like environmental exposure, material aging, electromagnetic interference, mechanical stress, and material fatigue. Harsh weather conditions, corrosion, and UV radiation can lead to physical damage, while prolonged exposure to electromagnetic fields can reduce efficiency [111]. On the other hand, stability refers to how consistently an antenna maintains its desired performance despite changing conditions. Factors like design robustness, thermal stability, mechanical stability, and material selection play a significant role in ensuring that the antenna operates efficiently under varying environmental, mechanical, or electrical stresses. In real-world applications, such as in satellite communication or remote sensing, both degradation and stability are critical to ensuring that antennas function reliably over extended periods, reducing maintenance needs and improving the system's overall lifespan [108].

6.8 Data Acquisition Band for Implantable Antenna

Another important aspect is the interaction of the MXene antenna with biological tissues during operation. Antennas designed for biomedical implants typically operate in specific frequency ranges, such as the Medical Implant Communication Service (MICS) band at 402–405 MHz or ISM bands like 2.4 GHz [112]. These frequencies ensure efficient communication with minimal energy loss, but the power levels must comply with regulatory standards for Specific Absorption Rate (SAR) to prevent tissue heating and damage [113]. Moreover, the miniaturization and flexibility of MXene antennas make them suitable for implantation in various anatomical locations, ensuring minimal interference with bodily functions. The flexibility of MXene combined with thin substrates allows the antenna to conform to body contours, improving both comfort and performance. Biocompatibility also extends to the antenna's ability to avoid immune rejection and chronic inflammation [114]. Proper surface treatments and material selection ensure non-immunogenic properties, reducing the risk of adverse immune responses. For instance, functionalizing MXene surfaces with biocompatible polymers can reduce the likelihood of protein adsorption, a precursor to immune activation. Long-term stability under implantation conditions is another essential factor. Continuous exposure to varying pH levels, enzymatic activities, and mechanical stresses necessitates robust material design to maintain performance and avoid degradation over time.

When designing MXene patch antennas for biomedical application offer excellent miniaturization and flexibility. Their inherent material properties, such as high electrical conductivity and tunable surface chemistry, allow the design of compact antenna that can operate efficiently even at small sizes. Additionally, MXenes can be fabricated on flexible substrates, making them suitable for conformal applications on irregular body surfaces. The dielectric constant of MXenes can be tailored by modifying their surface chemistry, allowing optimization for impedance matching, resonant frequency, and bandwidth, which are essential for efficient antenna operation. Additionally, MXenes exhibit low dielectric loss, ensuring minimal signal attenuation and energy dissipation when used in antennas. This low loss is especially important for biomedical applications where efficiency and energy conservation are paramount to prevent overheating or interference with body tissues [115], [116].

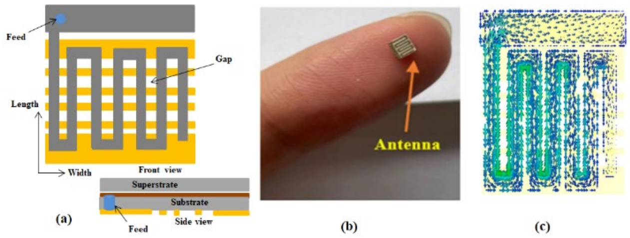

Figure 9. (a) Biomedical implantable antenna structure, (b) fabricated printing antenna for biomedical implant, (c) current distribution based on frequency [117].

6.9 Importance in Healing of Bone Fracture

Figure 10 represents various applications and studies on implantable antennas for monitoring and diagnosing fractured bones and damaged organs. Direct and indirect trauma can lead to bone fractures, as shown in Figure 6. The severity and type of fracture are determined by the extent of damage caused to the body and the bone. Severe trauma often results in fractures, which require extended biological healing. Restoring the original state of a bone necessitates continuous monitoring along with mechanical assistance [89].

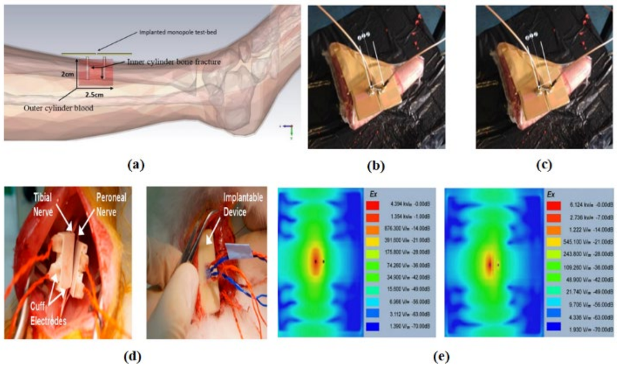

Figure 10. Highlights various aspects: (a) Detection of fractured bones, (b) Testing bone fracture healing, (c) Monitoring blood pressure inside the left ventricle, (d) Surgical procedure of an implantable antenna on rabbit skin, (e) Electric field distribution monitoring for damaged organs [89], [16], [118].

In orthopedic studies, X-rays are typically used to detect bone fractures and assess the condition of damaged bones. As part of advancements in medical technology, implantable antennas have emerged as a key area of research. Figure 10 (a) illustrates a system where two monopole antennas are attached to a metal plate to monitor the healing process of fractured bones [16]. The system employs highly conductive and dielectric materials. Blood's higher relative permittivity and conductivity compared to bone result in a larger wave number and increased attenuation of the electric field in the fractured bone area [89]. Figures 9 (c), 10 (c), and 10 (e) specifically represent the electric field distribution and the percentage of bone damage (ranging from 0% intact to 100% fractured). These in vivo tests demonstrate the use of a monopole antenna for tracking bone fracture healing and monitoring blood pressure in the left ventricle at a frequency of 1.8 GHz [16]. The antenna positioned on either side of the fracture assess the healing process by transmitting power between monopoles [89].

Additionally, an ultra-thin, electrically safe MXene patch antenna is explored as an implantable capacitive electrode arrays for monitoring marrow bones and the cortex. These electrodes collect electrocorticography signals and detect abnormalities [119], [120]. Figure 10 (d) and 10 (e) shows a surgical experiment conducted in a rabbit, where a three-centimeter incision was made on the back of its left hind limb to expose the sciatic nerve through the avascular fascicular junction based on the design of Figure 9 (a) and 9 (b). The antenna system was then used to record and stimulate peripheral nerve activity following hair removal from the thigh [121].

7. CHALLENGES

While MXenes hold great potential for biomedical applications, they face several challenges related to their oxidation, biocompatibility, and durability in a biological environment. Especially Ti_3C_2, are prone to oxidation when exposed to air, water, or biological fluids, leading to degradation of their properties, such as electrical conductivity and mechanical strength. Oxidation products can negatively affect device performance and may produce toxic byproducts. The cytotoxicity of MXenes depends on their composition, size, and functionalization. Non-functionalized MXenes may release ions or particles that could harm living tissues or cells. Inflammatory responses or immune system activation could occur if the material interacts poorly with biological systems. It may degrade or lose functionality due to interactions with biological fluids (pH, enzymes, salts), and mechanical stresses in dynamic biological environments, such as blood flow or tissue movement, can lead to structural failure. Functionalize the surface with groups like polymers, proteins, or biomolecules to protect MXene from oxidative degradation. It can be use biocompatible coatings such as hydrogels or thin films to isolate MXene from the biological environment. Attaching -OH, -COOH, or $-NH_2$ groups to the MXene surface to reduce cytotoxicity and enhance interaction with biological systems. Perform extensive in vitro and in vivo studies to evaluate MXene safety at various concentrations and exposure durations. It is possible to reduce material sensitivity by utilizing pH-sensitive coatings or buffers to stabilize MXenes in acidic or alkaline biological environments.

8. FUTURE PROSPECTS AND PROPOSED RESEARCH DIRECTION

MXenes are prone to oxidation in biological environments, affecting their electrical and mechanical properties over time. Limited studies on the long-term safety of MXenes in vivo, especially regarding chronic exposure. Potential cytotoxicity and immune responses require deeper investigation for implantable biomedical applications. Challenges in achieving efficient signal transmission through dense and heterogeneous biological tissues. Loss of signal strength due to tissue absorption and scattering. Optimize antenna design to reduce tissue absorption and enhance signal strength in high-loss environments. Investigate novel MXene composites with improved electromagnetic properties for better penetration. It is efficient for future research to develop advanced surface coatings (hydrogels, biopolymers) to mitigate cytotoxicity and improve compatibility with biological tissues.

9. CONCLUSION

This review highlights the significant potential of incorporating two-dimensional transition metal carbides (Ti_3C_2), into flexible patch antenna for next-generation wireless communication and biomedical implantable devices. MXene's unique combination of high electrical conductivity, tunable dielectric properties, and mechanical flexibility makes it a promising material for addressing the demands of 5G and other advanced applications. The review summarizes MXene synthesis techniques, emphasizing the importance of controlled synthesis for optimal performance. It also explores various integration strategies within the patch antenna structure and analyzes their impact on key antenna parameters. Finally, the review emphasizes the potential of MXene-based antenna for biomedical application due to their biocompatibility, tenability and antibacterial properties. Overall, this study provides a comprehensive overview of the latest advancements in MXene-enhanced patch antennas encouraging further research and development in this rapidly evolving field.

ACKNOWLEDGMENT

The author would like to express sincere gratitude to the Centre for Sustainability in Advanced Electrical and Electronic Systems (CSAEES), Faculty of Engineering, Built Environment and Information Technology, SEGi University, 47810 Petaling Jaya, Selangor, Malaysia, for providing the academic environment, research facilities, and continuous support throughout this study. The author also extends heartfelt appreciation to the colleagues whose valuable guidance, encouragement, and constructive feedback significantly contributed to the successful completion of this research. Their support and expertise have been invaluable in achieving the objectives of this work.

REFERENCES

[1] Y. Shao, L. Wei, X. Wu, C. Jiang, Y. Yao, B. Peng, H. Chen, J. Huangfu, Y. Ying, C. J. Zhang, and J. Ping, "Room-temperature high-precision printing of flexible wireless electronics based on MXene inks," *Nat. Commun*., vol. 13, no. 1, pp. 1–8, 2022.

[2] N. Papadopoulos et al., "For the Internet of Everything," *Nat. Electron.,* vol. 2, no. 12, pp. 3–8, 2019.

[3] S. Dang, O. Amin, B. Shihada, and M. Alouini, "What should 6G be," *IEEE Commun. Mag.,* vol. 58, no. 1, pp. 1–12, 2020.

[4] B. Decoupling and D. M. Patch, "Broadband decoupling network for dual-band microstrip patch antennas," IEEE Trans. *Antennas Propag*., vol. 65, no. 10, pp. 5595–5598, 2017.

[5] M. H. S. Alrashdan, Z. Al-Qudah, and M. Al Bataineh, "Microstrip patch antenna directivity optimization via Taguchi method," *Alexandria*

Engineering Journal, 2024, Art. no. 102923, doi: 10.1016/j.asej.2024.102923.

[6] K. Pan et al., "Multilayer graphene ink for wireless connectivity," *Nat. Commun*., no. 2018.

[7] J. Wu et al., "Facile synthesis of 3D graphene flowers for ultrasensitive and highly reversible gas sensing," *Adv. Funct. Mater*., 2016.

[8] S. Y. Cho, S. J. Kim, Y. Lee, J. S. Kim, W. B. Jung, H. W. Yoo, J. Kim, and H. T. Jung, "Highly enhanced gas adsorption properties in vertically aligned MoS_2 layers," *ACS Nano*, vol. 9, no. 9, pp. 9314–9321, 2015.

[9] A. K. Geim and K. S. Novoselov, "The rise of graphene," *Nat. Mater*., vol. 6, no. 3, pp. 183–191, 2007.

[10] S. Y. Cho, Y. Lee, H. J. Koh, H. Jung, J. S. Kim, H. W. Yoo, J. Kim, and H. T. Jung, "Superior chemical sensing performance of black phosphorus: comparison with MoS_2 and graphene," *Adv. Mater*., vol. 28, no. 32, pp. 7020–7028, 2016.

[11] J. Kimionis, A. Georgiadis, S. N. Daskalakis, and M. M. Tentzeris, "A printed millimetre-wave modulator and antenna array for backscatter communications at gigabit data rates," *Nat. Electron*., vol. 4, no. 6, pp. 439–446, June 2021.

[12] M. A. Seo, H. R. Park, S. M. Koo, D. J. Park, J. H. Kang, O. K. Suwal, S. S. Choi, P. C. M. Planken, G. S. Park, N. K. Park, Q. H. Park, and D. S. Kim, "Terahertz field enhancement by a metallic nano slit operating beyond the skin-depth limit," *Nat. Photonics*, vol. 3, no. 3, pp. 152–156, 2009.

[13] F. C. Walsh, "Electrode reactions in metal finishing," *Trans. Inst. Met. Finish*., vol. 69, no. 3, pp. 107–110, 1991.

[14] S. Lv, S. Ye, C. Chen, Y. Zhang, Y. Wu, Y. Wang, R. Tang, M. M. De Souza, X. Liu, and X. Zhao, "Reactive inkjet printing of graphene-based flexible circuits and radio frequency antennas," *J. Mater. Chem. C,* vol. 9, no. 38, pp. 13182–13192, 2021.

[15] M. Shalini and M. G. Madhan, "Design and analysis of a dual-polarized graphene-based microstrip patch antenna for terahertz applications," *Optik*, vol. 194, p. 163050, 2019.

[16] L. Lan, J. Zou, C. Jiang, B. Liu, L. Wang, and J. Peng, "Inkjet printing for electroluminescent devices: emissive materials, film formation, and display prototypes," *Front. Optoelectron*., vol. 10, no. 4, pp. 329–352, 2017.

[17] S. Symeonidis, W. G. Whittow, C. Panagamuwa, and M. Zecca, "An implanted antenna system for the monitoring of the healing of bone fractures," *Loughborough Antennas & Propagation Conference (LAPC)*, November 2015.

[18] A. Sarycheva, A. Polemi, Y. Liu, K. Dandekar, B. Anasori, and Y. Gogotsi, "2D titanium carbide (MXene) for wireless communication," *Sci. Adv*., vol. 4, no. 9, pp. eaau0920, Sep. 2018.

[19] N. Horiz et al., "Flexible two-dimensional MXene-based antennas," *Nanoscale Horizons*, vol. 8, pp. 309–319, 2023.

[20] M. Han, Y. Liu, R. Rakhmanov, C. Israel, M. A. S. Tajin, G. Friedman, V. Volman, A. Hoorfar, K. R. Dandekar, and Y. Gogotsi, "Solution-Processed $Ti_3C_2T_x$ MXene Antennas for Radio-Frequency Communication," *Adv. Mate*r., vol. 33, no. 1, p. 2003225, Jan. 2021.

[21] A. Mohan and N. Kumar, "Implantable antennas for biomedical applications: a systematic review," *Biomed. Eng. Online*, vol. 23, no. 1, pp. 87, 2024.

[22] Aliqab, I. Nadeem, and S. R. Khan, "A Comprehensive Review of In-Body Biomedical Antennas: Design, Challenges and Applications," *Micromachines*, vol. 14, no. 7, p. 1472, July 2023.

[23] M. Downes et al., "M5X4: A Family of MXenes," *ACS Nano*, vol. 17, no. 17, pp. 17158–17168, 2023.

[24] N. T. M. Mxene, "Research Progress of Novel Two-Dimensional Material MXene," *J. Inorg. Mater*., vol. 32, no. 6, pp. 561–570, 2017.

[25] R. Verma, A. Sharma, V. Dutta, A. Chauhan, D. Pathak, and S. Ghotekar, "Recent trends in synthesis of 2D MXene-based materials for sustainable environmental applications," *Emergent Mater*., vol. 7, pp. 35–62, 2024.

[26] K. Hantanasirisakul and Y. Gogotsi, "Electronic and Optical Properties of 2D Transition Metal Carbides and Nitrides (MXenes)," *Adv. Mater*., vol. 30, no. 52, Dec. 2018.

[27] P. He, M.-S. Cao, W.-Q. Cao, and J. Yuan, "Developing MXenes from Wireless Communication to Electromagnetic Attenuation," *Nano-Micro Lett*., vol. 13, no. 1, pp. 1–34, Apr. 2021.

[28] M. Mozafari and M. Soroush, "Surface functionalization of MXenes," *Mater. Adv*., vol. 2, no. 22, pp. 7277–7307, 2021.

[29] Z. Liu, G. Li, Y. Zhao, and X. Chen, "Surface Groups and Dielectric Properties of $Ti_3C_2T_x$ MXene Nanosheets after NH3•H2O Solvothermal Treatment under Different Temperatures," *Crystals*, vol. 13, no. 7, p. 1005, July 2023.

[30] B. Anasori, M. R. Lukatskaya, and Y. Gogotsi, "2D metal carbides and nitrides (MXenes) for energy storage," *Nature Reviews Materials*, vol. 2, no. 2, pp. 16098, Feb. 2017.

[31] B. Ahmed, J. Hossain, A. Al Parvez, A. Talukder, A. Al Mahmud, and T. Islam, "Recent Advancements of MXene/Nanocellulose-Based Hydrogel and Aerogel: A Review," *Adv. Eng. Sci. Res*., vol. 2300231, 2023.

[32] Y. Cui, J. Zhu, H. Tong, and R. Zou, "Advanced perspectives on MXene composite nanomaterials: Types synthetic methods, thermal energy utilization and 3D-printed techniques," *iScience,* vol. 26, no. 1, p. 105824, Jan. 2023.

[33] C. E. Shuck, M. Han, K. Maleski, K. Hantanasirisakul, S. J. Kim, J. Choi, W. E. B. Reil, and Y. Gogotsi, "Effect of Ti_3AlC_2 MAX Phase on Structure and Properties of Resultant $Ti_3C_2T_x$ MXene," *ACS Appl. Nano Mater*., vol. 2, pp. 3368–3376, 2019.

[34] M. Naguib, O. Mashtalir, J. Carle, V. N. Mochalin, M. W. Barsoum, and Y. Gogotsi, "Two-Dimensional Nanocrystals Produced by Exfoliation of Ti_3AlC_2," *Adv. Mater*., vol. 23, no. 37, pp. 4248–4253, 2011.

[35] S. Vasu, D. Verma, O. S. S. S, K. A. Reddy, G. Packirisamy, and U. K. S., "In Situ Ag-Seeded Lamellar Ti3C2 Nanosheets: An Electroactive

Interface for Noninvasive Diagnosis of Oral Carcinoma via Salivary TNF-α Sensing," *ACS Appl. Bio Mater.*, vol. 8, no. 1, pp. 420–434, Jan. 2025.

[36] F. Liu, A. Zhou, J. Chen, J. Jia, W. Zhou, and L. Wang, "Preparation of Ti_3C_2 and Ti_2C MXenes by fluoride salts etching and methane adsorptive properties," *Appl. Surf. Sci.*, vol. 416, pp. 781–789, Sep. 2017.

[37] Y. Gogotsi and B. Anasori, "The Rise of MXenes," *ACS Nano*, vol. 13, no. 8, pp. 8491–8494, Aug. 2019.

[38] K. R. G. Lim, M. Shekhirev, B. C. Wyatt, B. Anasori, Y. Gogotsi, and Z. W. Seh, "Fundamentals of MXene synthesis," *Nat. Synth.*, vol. 1, no. 8, pp. 601–614, Aug. 2022.

[39] O. Mashtalir, M. Naguib, V. N. Mochalin, Y. Dall'Agnese, M. Heon, M. W. Barsoum, and Y. Gogotsi, "Intercalation and delamination of layered carbides and carbonitrides," *Nat. Commun.*, vol. 4, p. 1716, Apr. 2013.

[40] A. T. Li et al., "Fluorine-Free Synthesis of High-Purity $Ti_3C_2T_x$ (T=OH, O) via Alkali Treatment," *Angew. Chem. Int. Ed.*, vol. 57, no. 19, pp. 5545–5549, 2018.

[41] A. Thakur et al., "Step-by-Step Guide for Synthesis and Delamination of $Ti_3C_2T_x$ MXene," *Small Methods*, vol. 7, no. 8, p. 2300030, Aug. 2023.

[42] I. Ali, M. Faraz, U. Din, and Z. Gu, "MXenes thin films: From fabrication to their applications," *Molecules*, vol. 27, no. 15, p. 4925, Aug. 2022.

[43] X. Yu, X. Cai, H. Cui, S.-W. Lee, X.-F. Yu, and B. Liu, "Fluorine-free preparation of titanium carbide MXene quantum dots with high near-infrared photothermal performances for cancer therapy," *Nanoscale*, vol. 9, no. 45, pp. 17859–17864, Nov. 2017.

[44] Q. Xue, H. Zhang, M. Zhu, Z. Pei, H. Li, Z. Wang, Y. Huang, Y. Huang, Q. Deng, J. Zhou, S. Du, Q. Huang, and C. Zhi, "Photoluminescent Ti_3C_2 MXene Quantum Dots for Multicolor Cellular Imaging," *Advanced Materials*, vol. 29, no. 15, Feb. 2017.

[45] G. Xu, Y. Niu, X. Yang, Z. Jin, Y. Wang, and Y. Xu, "Preparation of $Ti_3C_2T_x$ MXene-Derived Quantum Dots with White/Blue-Emitting Photoluminescence and Electrochemiluminescence," *Adv. Mater.*, vol. 30, no. 30, pp. 1–7, July 2018.

[46] M. S. Carey and M. W. Barsoum, "Scalable and sustainable production of Ti_3C_2Tz MXene and fluorine recovery from wastewater through cryolite precipitation," *RSC Adv.*, vol. 12, no. 47, pp. 30846–30850, Oct. 2022.

[47] K. Grabowski, T. Strączek, and T. Uhl, "Temperature Evolution of Composition, Thermal, Electrical and Magnetic Properties of $Ti_3C_2T_x$-MXene," *Materials*, vol. 17, no. 10, p. 2199, May 2024.

[48] Y. Peng, P. Cai, L. Yang, Y. Liu, L. Zhu, Q. Zhang, J. Liu, Z. Huang, and Y. Yang, "Theoretical and Experimental Studies of Ti_3C_2 MXene for Surface-Enhanced Raman Spectroscopy-Based Sensing," *ACS Omega*, vol. 5, no. 41, pp. 26486–26496, Oct. 2020.

[49] H. Hu, S. Wang, Y. Zhang et al., "MXene-based electromagnetic interference shielding materials: A leap from fundamental research to intelligent customization," *Small,* vol. 22, no. 13, 2026, Art. no. 2505417, doi: 10.1002/smll.202505417.

[50] Q. Gao, X. Wang, D. W. Schubert, and X. Liu, "Review on polymer/MXene composites for electromagnetic interference shielding applications," *Advanced Nanocomposites*, 2023, Art. no. 11.002, doi: 10.1016/j.adna.2023.11.002.

[51] G. Kaur, A. Singh, D. Mittal, Prince, A. Kaur, P. Panday, and E. Sidhu, "Performance analysis of conductive patch materials for the design and fabrication of microstrip patch antennas," *in Progress In Electromagnetics Research Symposium* - Spring (PIERS), St. Petersburg, Russia, 2017.

[52] A. S. Savoia et al., "An alternative material for transparent antennas for commercial and medical applications," *Microw. Opt. Technol. Lett.*, vol. 59, no. 4, pp. 773–777, Apr. 2017.

[53] S.-H. Wi, Y.-S. Lee, and J.-G. Yook, "Wideband microstrip patch antenna with U-shaped parasitic elements," *IEEE Trans. Antennas Propag.*, vol. 55, no. 4, pp. 1196–1199, Apr. 2007.

[54] M. M. Jadhav and J. N. Shinde, "Review of Impedance Bandwidth Enhancement Techniques of Microstrip Patch Antenna," *Int. J. Appl. Eng. Res.*, vol. 19, no. 2, pp. 140–149, 2024.

[55] P. A. Kashyap, K. Sarmah, I. Dakua, and S. Baruah, "Gain and bandwidth enhancement of slotted microstrip antenna using metallic nanofilms for WLAN applications," *J. King Saud Univ. - Sci.*, vol. 35, no. 1, p. 102374, Jan. 2023.

[56] N. A. Malik, P. Sant, T. Ajmal, and M. Ur-Rehman, "Implantable antennas for bio-medical applications," *IEEE J. Electromagn., RF Microw. Med. Biol.*, vol. 5, no. 1, pp. 84–96, Mar. 2021.

[57] M. H. Reddy, D. R. Sreenivasulu, D. S. Shankar, and S. T. Niba, "Microstrip Patch Antenna Design for SAR Reduction in Human Head Using Slotting Technique," *Int. J. Innov. Sci. Eng. Technol.*, vol. 2, no. 7, pp. 99–102, July 2017.

[58] P. Banerjee and T. Bezboruah, "Comparative study of transmission line and cavity model of rectangular microstrip antenna," *Int. J. Nat. Sci. Res.*, vol. 3, no. 6, pp. 76–82, June 2015.

[59] M. R. Hire and C. S. Ahire, "A Review on Microstrip Patch Antenna Design and its Applications," in *Proceedings of the 3rd International Conference on Contents, Computing & Communication (ICCCC*-2022), 2022.

[60] T. Tewary, S. Maity, S. Mukherjee, A. Roy, P. P. Sarkar, and S. Bhunia, "High gain miniaturized super-wideband microstrip patch antenna," *Int. J. Commun. Syst.*, vol. 35, no. 11, pp. e5181, 2022.

[61] M. K. Khandelwal, B. K. Kanaujia, and S. Kumar, "Defected Ground Structure: Fundamentals, Analysis, and Applications in Modern Wireless Trends," *Int. J. Antennas Propag.*, vol. 2017, pp. 1–22, 2017.

[62] T. March et al., "2007 Index IEEE Transactions on Antennas and Propagation," *IEEE Trans. Antennas Propag.*, vol. 55, no. 12, pp. 3750–3808, 2007.
[63] A. H. Lokman, P. J. Soh, S. N. Azemi, H. Lago, S. K. Podilchak, S. Chalermwisutkul, M. F. Jamlos, A. A. Al-Hadi, P. Akkaraekthalin, and S. Gao, “A Review of Antennas for Picosatellite Applications,” *International Journal of Antennas and Propagation*, vol. 2017, Art. no. 4940656, pp. 1–17, 2017, doi: 10.1155/2017/4940656.
[64] W. Zhu, Z. Gao, Z. Meng, C. Wang, Y. Li, C. Wang, and Y. Jia, “Research and Design of Radiofrequency Antenna on LCD,” *International Journal of Antennas and Propagation,* vol. 2022, Art. no. 5320561, pp. 1–7, 2022, doi: 10.1155/2022/5320561.
[65] Y. Mi, W. Liu, Y. Peng, L. Deng, B. Shu, X. Wang, and S. Li, “Research on low-profile directional flexible antenna with 3D coplanar waveguide for partial discharge detection,” *Micromachines,* vol. 16, no. 3, p. 253, 2025, doi: 10.3390/mi16030253.
[66] S. Douhi, S. Labihi, A. Eddiai, S. Lakrit, M. El Achaby, and A. J. A. Al-Gburi, “Design, characterization, and electromagnetic performance of a flexible wideband RF antenna using composite materials,” *J. Sci. Adv. Mater. Devices*, vol. 9, no. 4, p. 100847, 2024, doi: 10.1016/j.jsamd.2024.100847.
[67] X. Li, Y. Qian, and T. Liu, “Enhanced lithium and electron diffusion of $LiFePO_4$ cathode with two-dimensional Ti_3C_2 MXene nanosheets,” *J. Mater. Sci.*, vol. 53, no. 15, pp. 11078–11090, Aug. 2018.
[68] P.-Y. Chen and L. J. Guo, "Inkjet-printed invisible antenna facilitates next-generation wireless communication," *Device*, vol. 2, no. 2, p. 100289, 2024.
[69] G. Karles and H. Dante, "Print Quality Considerations in Ink Jet Printing in Industrial Applications," presented at the *International Conference on Digital Production Printing and Industrial Applications*, 2001, pp. 346–350.
[70] C. Gadea, Q. Hanniet, and A. Lesch, “Aqueous metal–organic solutions for YSZ thin film inkjet deposition,” *J. Mater. Chem. C*, vol. 5, pp. 6021–6029, 2017.
[71] W. Yang, X. Cheng, Z. Guo, Q. Sun, J. Wang, and C. Wang, “Design, fabrication and applications of flexible RFID antennas based on printed electronic materials and technologies,” *J. Mater. Chem. C*, vol. 11, no. 2, pp. 406–425, Jan. 2023.
[72] T. Inui, H. Koga, M. Nogi, N. Komoda, and K. Suganuma, “A miniaturized flexible antenna printed on a high dielectric constant nanopaper composite,” *Adv. Mater.,* vol. 27, no. 6, pp. 1112–1116, Feb. 2015.
[73] M. L. Scarpello, I. Kazani, C. Hertleer, H. Rogier, and D. V. Ginste, “Stability and efficiency of screen-printed wearable and washable antennas,” *IEEE Antennas Wireless Propag. Lett.*, vol. 11, pp. 838–841, 2012.
[74] H. Shahariar, H. Soewardiman, C. A. Muchler, J. J. Adams, and J. S. Jur, "Porous textile antenna designs for improved wearability," *Smart Materials and Structures*, vol. 27, no. 5, p. 055018, 2018.
[75] Y. Zhou, S. Soltani, B. M. Li, Y. Wu, I. Kim, H. Soewardiman, D. H. Werner, and J. S. Jur, “Direct-write spray coating of a full-duplex antenna for e-textile applications,” *Micromachines,* vol. 11, no. 12, pp. 1–15, Dec. 2020.
[76] O. Niksan, L. Bi, Y. Gogotsi, and M. H. Zarifi, "MXene-based kirigami designs: showcasing reconfigurable frequency selectivity in microwave regime," *Nature Communications*, vol. 15, no. 1, p. 7793, September 2024.
[77] L. C. T. Cao, C.-A. Jong, S.-H. Hsu, and S.-F. Tseng, “A simple approach to MXene micropatterning from molecularly driven assembly,” *ACS Omega*, vol. 6, no. 50, pp. 35866–35875, Dec. 2021.
[78] D. N. Ampong, E. Agyekum, F. O. Agyemang, K. Mensah-Darkwa, A. Andrews, and R. K. Gupta, “MXene: fundamentals to applications in electrochemical energy storage,” *Discover Nano*, vol. 18, no. 1, p. 3, 2023.
[79] S. Ganesan, K. R. Ethiraj, and M. K. Kesarla, Biomedical Applications of MXenes. *Springer International Publishing,* 2023. doi: 10.1007/978-3-031-05006-0.
[80] S. Kim and J. Byun, "Research Trends in Electromagnetic Shielding using MXene-based Composite Materials," *Korean Powder Metall. Inst.*, vol. 31, no. 1, pp. 57–76, 2024.
[81] W. Zhao et al., “2D Titanium carbide printed flexible ultra-wideband monopole antenna for wireless communications,” *Nat. Commun.*, vol. 14, no. 1, pp. 1–10, Jan. 2023.
[82] M. Naguib, M. W. Barsoum, and Y. Gogotsi, "Ten years of progress in the synthesis and development of MXenes," *Adv. Mater.*, vol. 33, no. 39, p. 2103393, Aug. 2021.
[83] M. Han, C. E. Shuck, R. Rakhmanov, D. Parchment, B. Anasori, C. M. Koo, G. Friedman, and Y. Gogotsi, “Beyond $Ti_3C_2T_x$: MXenes for Electromagnetic Interference Shielding,” *ACS Nano*, vol. 14, no. 4, pp. 5008–5016, 2020.
[84] B. Xia, Z. Wang, and T. Wang, "Bridging sheet size controls densification of MXene films for robust electromagnetic interference shielding," *iScience*, vol. 25, no. 9, p. 105001, Sep. 2022.
[85] Z. Song, Y. Wang, Y. Shi, and X. Zheng, "A miniaturized dual-band circularly polarized implantable antenna for use in hemodialysis," *Sensors*, vol. 24, no. 14, p. 4743, Jul. 2024.
[86] Y. Li, X. Tian, S.-P. Gao, L. Jing, K. Li, H. Yang, F. Fu, J. Y. Lee, Y.-X. Guo, J. S. Ho, and P.-Y. Chen, "Reversible crumpling of 2D titanium carbide (MXene) nanocoatings for stretchable electromagnetic shielding and wearable wireless communication," *Adv. Funct. Mater.*, vol. 30, no. 5, p. 1907451, 2020.
[87] K. S. Patil and E. Rufus, "A review on antennas for biomedical implants used for IoT based health care," *Sensor Review*, vol. 40, no. 2, pp. 273–280, 2020.
[88] A. R. Khan, V. Luckose, M. F. Kobir, N. F. H. Abdul Razak, M. A. Islam, and M. M. Rahman, “Wearable and Implantable Devices in Chronic Disease Management: Addressing Emerging

Challenges", *Jmeditec*, vol. 4, no. 1, pp. 1–8, Aug. 2025.

[89] A. Sondaş and M. H. B. Uçar, "An implantable microstrip antenna design for MICS-band biomedical applications," *Turkish Journal of Electrical Engineering & Computer Sciences*, vol. 24, no. 4, pp. 2267–2273, 2016.

[90] M. T. Islam, Y. Qiblawey, F. Musharavati, and E. Z. Nezhad, "Review on Medical Implantable Antenna Technology and Imminent Research Challenges," *Sensors*, vol. 21, no. 9, pp. 3163, May 2021.

[91] M. Gallieni et al., "Clinical practice guideline on peri- and postoperative care of arteriovenous fistulas and grafts for haemodialysis in adults," *Nephrology Dialysis Transplantation,* vol. 35, no. 1, pp. 1–10, Jan. 2020, doi: 10.1093/ndt/gfz072.

[92] J. Zhang, H. Wang, H. Haidari, R. Das, "A Compact Dual-Band Implantable Antenna for Wireless Biotelemetry in Arteriovenous Grafts," *IEEE Trans. Antennas Propag*., vol. 71, pp. 1234–1243, Mar. 2023.

[93] Y. Fan, H. Liu, X. Liu, Y. Cao, Z. Li, and M. M. Tentzeris, "Novel coated differentially fed dual-band fractal antenna for implantable medical devices," *IET Microwaves, Antennas & Propagation*, vol. 14, pp. 199–208, 2019.

[94] V. Kaim, B. K. Kanaujia, and K. Rambabu, "Quadrilateral spatial diversity circularly polarized MIMO cubic implantable antenna system for biotelemetry," *IEEE Trans. Antennas Propag*., vol. 69, no. 3, pp. 1260–1272, Mar. 2021.

[95] C. Xu, Y. Fan, and X. Liu, "A Circularly Polarized Implantable Rectenna for Microwave Wireless Power Transfer," *Micromachines*, vol. 13, no. 1, p. 121, Jan. 2022.

[96] S. M. Asif, A. Iftikhar, B. D. Braaten, D. L. Ewert, and K. Maile, "A wide-band tissue numerical model for deeply implantable antennas for RF-powered leadless pacemakers," *IEEE Access*, vol. 7, pp. 31031–31042, Mar. 2019, doi: 10.1109/ACCESS.2019.2902981.

[97] I. Ben Mabrouk, T. Djerafi, M. Zada, and F. Faisal, "An ultra-miniaturized antenna with ultra-wide bandwidth for future cardiac leadless pacemaker," *IEEE Trans. Antennas Propag*., vol. 70, no. 7, pp. 5923–5928, March, 2022.

[98] P. Bose, A. L. I. Khaleghi, and S. Mahmood, "Evaluation of data telemetry for future leadless cardiac pacemaker," *IEEE Access,* vol. 7, pp. 157933–157945, 2019, doi: 10.1109/ACCESS.2019.2950146.

[99] D. Sharma, B. K. Kanaujia, V. Kaim, R. Mittra, R. K. Arya, and L. Matekovits, "Design and implementation of compact dual-band conformal antenna for leadless cardiac pacemaker system," *Sci. Rep.*, vol. 12, no. 1, pp. 3165, Mar. 2022, doi: 10.1038/s41598-022-06904-2.

[100] D. Sharma, B. K. Kanaujia, S. Kumar, K. Rambabu, and L. Matekovits, "Low-loss MIMO antenna wireless communication system for 5G cardiac pacemakers," *Sci. Rep.,* vol. 13, no. 9557, 2023, doi: 10.1038/s41598-023-36209-x.

[101] I. I. Smolyaninov, Q. Balzano, V. N. Smolyaninova, and D. Soloviova, "Electromagnetic signal propagation through lossy media via surface electromagnetic waves," *Nanophotonics*, vol. 13, no. 7, pp. 1005–1015, 2023, doi: 10.1515/nanoph-2023-0668.

[102] A. Shabana, A. El-Bakry, and S. Mahdy, "Implantable antenna for biomedical applications: electromagnetic, SAR, and thermal performance evaluation," *Sci. Rep*., vol. 15, no. 1, p. 35404, 2025, doi: 10.1038/s41598-025-21600-7.

[103] Z.-J. Yang, L. Zhu, and S. Xiao, "An implantable circularly polarized patch antenna design for pacemaker monitoring based on quality factor analysis," *IEEE Trans. Antennas Propag.,* vol. 66, no. 10, pp. 5180–5192, Oct. 2018.

[104] I. Dove, "Analysis of radio propagation inside the human body for in-body localization purposes," Master's thesis, Univ. *Twente, Enschede*, Netherlands, 2014.

[105] D. Nikolayev, Z. Sipus, M. Bosiljevac, W. Joseph, M. Zhadobov, R. Sauleau, L. Martens, and A. K. Skrivervik, "Optimal frequency of operation and radiation efficiency limitations of implantable antennas*," IEEE Trans. Antennas Propag*., vol. 68, no. 3, pp. 1749–1761, Mar. 2020.

[106] M. E. Marchwiany, M. Birowska, M. Popielski, J. A. Majewski, and A. M. Jastrzębska, "Surface-Related Features Responsible for Cytotoxic Behavior of MXenes Layered Materials Predicted with Machine Learning Approach," *Materials,* vol. 13, no. 14, pp. 3083, June. 2020, doi: 10.3390/ma13143083.

[107] S. N. Sankar, G. Araujo, J. Fernandes, F. Cerqueira, P. Alpuim, A. R. Ribeiro, F. Lebre, E. Alfaro-Moreno, E. Placidi, S. Marras, and A. Capasso, "Eco-friendly production of 2D Ti3C2Tx MXene and cytotoxicity mitigation toward biomedical applications," *Adv. Mater. Interfaces*, vol. 2400203, pp. 1–12, 2024, doi: 10.1002/admi.202400203.

[108] Y. Hu, F. Wang, H. Ye, J. Jiang, S. Li, B. Dai, J. Li, J. Yang, X. Song, J. Zhang, Y. Xie, L. Gao, and D. Yang, "MXene-based flexible electronic materials for wound infection detection and treatment," *npj Flexible Electronics*, vol. 8, no. 1, p. 30, Dec. 2024.

[109] A.-C. Bunea, V. Dediu, E. A. Laszlo, F. Pistrițu, M. Carp, F. S. Iliescu, O. N. Ionescu, and C. Iliescu, "E-Skin: The Dawn of a New Era of On-Body Monitoring Systems," *Micromachines*, vol. 12, no. 9, p. 1091, 2021.

[110] S. G. Kirtania, A. W. Elger, M. R. Hasan, A. Wisniewska, K. Sekhar, T. Karacolak, and P. K. Sekhar, "Flexible Antennas: A Review," *Micromachines*, vol. 11, pp. 847, Sept. 2020, doi: 10.3390/mi11090847.

[111] S. Shankar, B. B. Murphy, N. Driscoll, M. Shekhirev, S. Street, and S. Hall, "Effect of the deposition process on the stability of $Ti_3C_2T_x$ MXene films for bioelectronics," *2D Materials*, vol. 10, no. 4, pp. 044001, 2023.

[112] S. R. Averbeck, D. Xu, B. B. Murphy, K. Shevchuk, S. Shankar, M. Anayee, M. D. T. Torres, M. S. Beauchamp, C. de la Fuente-Nunez, Y. Gogotsi, and F. Vitale, "Stability of Ti3C2Tx

MXene Films and Devices under Clinical Sterilization Processes," *ACS Nano,* vol. 17, pp. 9442–9454, May 2023.

[113] M. Usluer and B. Cetindere, "Compact implantable antenna design for MICS and ISM band biotelemetry applications," *Microwave Opt. Technol. Lett.*, vol. 62, no. 4, pp. 1581–1587, 2020, doi: 10.1002/mop.32185.

[114] K. Guido and A. Kiourti, "Wireless Wearables and Implants: A Dosimetry Review," *Bioelectromagnetics,* vol. 41, no. 1, pp. 3–20, Jan. 2020, doi: 10.1002/bem.22240.

[115] Y. Onuki, U. Bhardwaj, F. Papadimitrakopoulos, and D. J. Burgess, "A review of the biocompatibility of implantable devices: current challenges to overcome foreign body response," J. *Diabetes Sci. Technol*., vol. 2, no. 6, pp. 1003–1015, Nov. 2008.

[116] S. A. Mirkhani, A. S. Zeraati, E. Aliabadian, M. Naguib, and U. Sundararaj, "High Dielectric Constant and Low Dielectric Loss via Poly(vinyl alcohol)/Ti3C2Tx MXene Nanocomposites," *ACS Applied Materials & Interfaces,* vol. 11, pp. 18599–18608, 2019, doi: 10.1021/acsami.9b00393.

[117] A. Maleki, M. Ghomi, N. Nikfarjam, M. Akbari, E. Sharifi, M.-A. Shahbazi, M. Kermanian, M. Seyedhamzeh, E. N. Zare, M. Mehrali, O. Moradi, F. Sefat, V. Mattoli, P. Makvandi, and Y. Chen, "Biomedical applications of MXene-integrated composites: regenerative medicine, infection therapy, cancer treatment, and biosensing," *Adv. Funct. Mater.*, vol. 32, no. 34, pp. 2203430, Aug. 2022, doi: 10.1002/adfm.202203430.

[118] F. Yang, L. Zhaonan, Q. Lin, S. Wanting, and L. Gaosheng, "A compact and miniaturized implantable antenna for ISM band in wireless cardiac pacemaker system," *Scientific Reports*, vol. 12, p. 238, 2022, doi: 10.1038/s41598-021-04404-3.

[119] A. Shon, J.-U. Chu, J. Jung, H. Kim, and I. Youn, "An implantable wireless neural interface system for simultaneous recording and stimulation of peripheral nerve with a single cuff electrode," *Sensors*, vol. 18, no. 1, pp. 1–26, Jan. 2018.

[120] C. Chen, M. Xue, Y. Wen, G. Yao, Y. Cui, F. Liao, Z. Yan, L. Huang, S. A. Khan, M. Gao, T. Pan, H. Zhang, W. Jing, D. Guo, S. Zhang, H. Yao, X. Zhou, Q. Li, Y. Xia, and Y. Lin, "A ferroelectric ceramic/polymer composite-based capacitive electrode array for in vivo recordings," *Adv. Healthcare Mater*., vol. 6, no. 6, pp. 1700305, May 2017, doi: 10.1002/adhm.201700305.

[121] I. S. Grønningsæter, A. B. Ahmed, N. Vetti, S. Johansen, Ø. Bruserud, and H. Reikvam, "Bone marrow abnormalities detected by magnetic resonance imaging as initial sign of hematologic malignancies," *Clin. Pract.*, vol. 8, pp. 63–66, 2018.